Colloid Polym Sci (2014) 292:107–113
DOI 10.1007/s00396-013-3050-6

ORIGINAL CONTRIBUTION

Facile preparation of pH-sensitive poly(acrylic acid-co-acrylamide)/SiO_2 hybrid hydrogels with high strength by in situ frontal polymerization

Shengfang Li · Hanlin Wang · Weidong Huang · Xianli Liu

Received: 28 April 2013 / Revised: 17 July 2013 / Accepted: 5 August 2013 / Published online: 29 August 2013

Abstract A series of poly(acrylic acid-co-acrylamide) (PAA)/SiO_2 hybrid hydrogels were prepared by in situ frontal polymerization. It was found that the increase in the concentration of SiO_2 nanoparticles could lead to the increase in front velocity (V_f) and the highest front temperature (T_{max}). This may be attributed to the fact that SiO_2 nanoparticles could increase the liquid viscosity of reaction mixture. The obtained PAA/SiO_2 hybrid hydrogels were characterized by SEM and Fourier transform infrared spectroscopy spectrum and swelling measurements. The pH-sensitive swelling behaviors showed that the prepared PAA/SiO_2 hybrid hydrogel had high pH sensitivity in different pH buffer solutions. Mechanical property test indicated that the PAA/SiO_2 hybrid hydrogels exhibited a high compressive strength while remaining a high swelling radio (SR). The maximum of compressive strength and SR of the hybrid hydrogel may reach 42.6 kPa and 17.8, respectively, which was much higher than that of pure PAA hydrogel.

Keywords SiO_2 nanoparticles · Hybrid hydrogel · Frontal polymerization · Compressive strength

Introduction

In recent years, environmental-sensitive hydrogels have gained considerable attention because they can exhibit volume or phase transition in response to external environmental stimuli such as pH, temperature, light, electronic and magnetic field, etc. These hydrogels mainly include pH, temperature, light, electronic- and magnetic-sensitive hydrogels, etc. They have great potential application in drug delivery carriers, tissue engineering, artificial muscles, biosensors, adsorbents and bioseparation, etc. [1]. The polyacrylate-based hydrogel is one of the most important pH-sensitive hydrogels, which have many acidic pendent groups in the hydrogel networks. Considering the dissociation of acidic groups and the influx of counter ions, the ionic concentration in the hydrogels is often higher than that in the surrounding solution. Thus, it leads to a difference in osmotic pressure between the hydrogel and solution, which causes the solution molecules to penetrate into the hydrogel and leads to a high degree of swelling of hydrogels. However, this high osmotic pressure often leads to break the hydrogel networks under the effect of internal stress. Therefore, this inherent drawback limits the application of pH-sensitive hydrogels. To overcome this shortcoming, it is necessary to enhance the strength of pH-sensitive hydrogels while remaining their good pH sensitivity [2, 3]. Up till now, some studies have attempted to improve the mechanical strength of pH-sensitive hydrogels by introducing interpenetrating polymer network [4, 5], hydrophobic monomers [6] or inorganic nanoparticles into hydrogels and so on [7–9].

It is well known that frontal polymerization (FP) is a reaction model of converting monomer into polymer via a localized and propagating reaction in a tube, which presents obvious advantage with a fast and efficient way to produce the polymers [10]. Many polymers and polymeric hydrogels, such as polyurethane, poly(*N*-methylolacrylamide)/polyhedral oligomeric silsesquioxane, monolithic macroporous polymers, poly(*N*-methylolacrylamide)/polymethylacryamide hybrids, poly(HPA-*co*-VeoVa10) amphiphilic gels, and poly(*N*-isopropylacrylamide) hydrogels have been prepared by FP [11–20]. In our previous research, we rapidly prepared poly(acrylic acid-co-acrylamide) (PAA) hydrogels via FP for dye removal [21].

S. Li (✉) · H. Wang · W. Huang
School of Chemical and Material Engineering, Hubei Polytechnic University, Huangshi 435003, People's Republic of China
e-mail: lishengf_@163.com

X. Liu
Hubei Key Laboratory of Mine Environmental Pollution Control and Remediation, Hubei Polytechnic University, Huangshi 435003, People's Republic of China

In this study, new pH-sensitive PAA/SiO_2 hybrid hydrogels were prepared by in situ FP. SiO_2 nanoparticles were rapidly embedded into PAA hydrogel matrix to enhance the mechanical strength of PAA hydrogels via simple FP technique to avoid aggregation of SiO_2 nanoparticles during the polymerization of monomers (see Fig. 1). The obtained pH-sensitive PAA/SiO_2 hybrid hydrogels were characterized by SEM and Fourier transform infrared spectroscopy (FTIR). The pH sensitivity and compressive strength of PAA/SiO_2 hybrid hydrogels were also investigated in details.

Experimental

Materials

Acrylic acid (AAc) was purchased from Tianjin Chemical Reagent Co. (Tianjin, China) and was distilled before use. Acrylamide (AM), potassium persulfate (KPS), *N*,*N*′-methylenebisacrylamide (MBA), and *N*,*N*′-dimethylformamide (DMF) was purchased from Shanghai Reagent Co. (Shanghai, China). SiO_2 nanoparticles were purchased from Haitai Nano-materials Co. (Nanjing, China). The Brunauer–Emmett–Teller surface area is 220 m^2 g^{-1}. The average diameter of nanoparticles is about 500 nm. All the reagents were of analytical grade and used as received without any further purification.

Preparation of hybrid hydrogels by in situ FP

First, the appropriate amount of SiO_2 nanoparticles was sonicated in DMF and mixed with AAc, AM, MBA, and KPS. Then the mixture was placed for 5 min and was poured into a glass test tube (20 mL; 12.8 mm diameter). To monitor the temperature change, a K-type thermocouple connected to a digital thermometer was immersed into the mixture at about 3 cm from the bottom of the tube. The filled tube was clamped into a holder 1 cm from the top of the tube and kept at ambient temperature. The upper side of the mixture composed of monomers and SiO_2 nanoparticles was heated by a soldering iron until the hot propagating front commenced. After the completion of the reaction, the sample was removed from the tube, cut into small pieces, and immersed in deionized water over 3 days to dissolve soluble materials. The obtained hybrid hydrogel products were dried in vacuum at 50 °C to a constant weight and stored for further use. The feed composition of samples during in situ FP was listed and designed as FPn in Table 1.

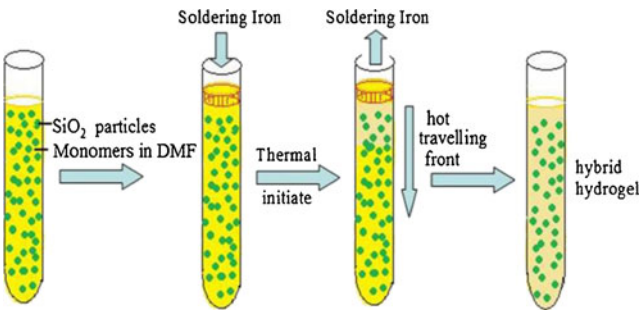

Fig. 1 Schematic representation of the preparation of PAA/SiO_2 hybrid hydrogels by in situ FP

Table 1 Feed composition of samples during the in situ frontal polymerization

Samples	AAc/AM (wt/wt)	MBA (wt.%)	KPS (wt.%)	SiO_2 (g mL^{-1})
FP0	3:7	1	0.1	0
FP1	3:7	1	0.1	0.010
FP2	3:7	1	0.1	0.016
FP3	3:7	1	0.1	0.022
FP4	3:7	1	0.1	0.025

Velocity and temperature measurements

The front velocities were confirmed by measuring the front position as a function of time. Temperature profiles were determined by measuring the temperature at a fixed point as a function of time, using a K-type thermocouple and converted to spatial ones using front velocities. After the completion of the reaction, the samples were cooled to room temperature and removed from the tube for further investigation.

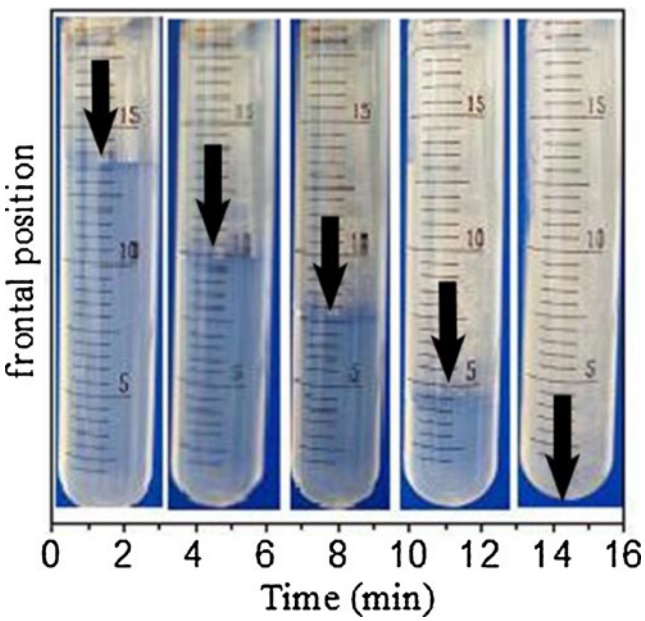

Fig. 2 The visual images of propagating front of PAA/SiO_2 hybrid hydrogel (the height of the tube is 10 cm and inner diameter of the tube is 12.8 mm)

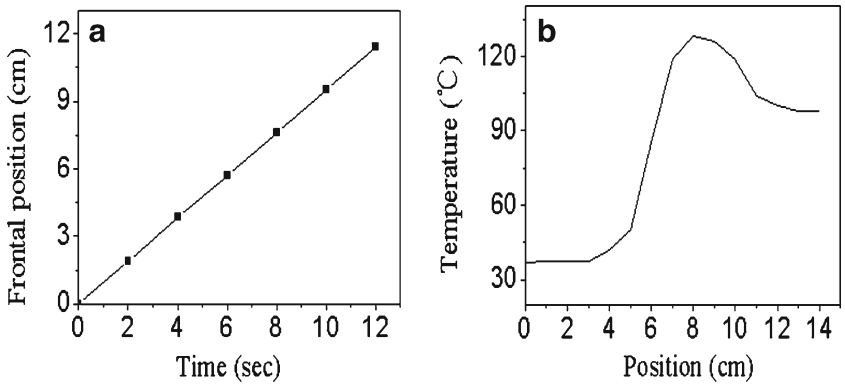

Fig. 3 Front positions versus time (**a**) and front temperature profile (**b**) for FP2 hybrid hydrogel

Characterization and mechanical properties of hybrid hydrogels

Morphology of dry hydrogels was observed by SEM (JSM-5610LV) with an acceleration voltage of 10 kV. The equilibrium-swollen gels were frozen by liquid nitrogen for 6 h, freeze dried, and fractured. The fractured specimens were covered with gold vapor, and then the morphology of the fractured surface of the dry hydrogel was observed by SEM. FTIR spectroscopy was used to confirm the structure of composite hydrogels. The composite hydrogel samples were analyzed on a Bruker EQUNINOX FTIR spectrophotometer in the region of 400–4,000 cm^{-1}. Before the measurements, the dried composite hydrogel samples were crushed down (KBr, pellet). Compressive strength of the swollen hydrogels was tested using a self-prepared equipment described earlier [6]. Compressive strength (Ss) was calculated as follows:

$$Ss = F/S \quad (1)$$

Where, F is force applied and S is the surface area of the swollen hydrogel.

Swelling studies of hybrid hydrogels

The swelling properties of the as-prepared hybrid hydrogels were performed by gravimetric analysis. Briefly, the dry hybrid hydrogel was immersed in the swelling medium at 25 °C. At regular time intervals, the gels were removed from the medium and the weight of the swollen hybrid hydrogel was determined after the removal of the surface water through blotting with filter paper. The measurements were continued until the weight of hydrogels reached a constant value. The swelling ratio (SR) was calculated by the following equation:

$$SR = (W_t - W_0)/W_0 \quad (2)$$

Where, W_t is the mass of the swollen hydrogels at t, and W_0 is the initial mass of dry hydrogel. All of the experiments were triplicated.

Results and discussion

FP and influence of SiO_2 nanoparticles

The PAA/SiO_2 hybrid hydrogels were prepared by in situ FP. To obtain PAA/SiO_2 hybrid hydrogels with homogeneous dispersion of SiO_2 nanoparticles, SiO_2 nanoparticles were first sonicated in DMF and then mixed with AAc, AM, and KPS to carry out in situ FP experiments. Figure 2 presents the typical images of propagating fronts of the PAA/SiO_2 hybrid hydrogel. An interface between the hybrid and mixture composed of unreacted monomers and SiO_2 nanoparticles can be obviously seen. The upper homogeneous white layer was PAA/SiO_2 hybrid, and the lower transparent layer was the mixture consisted of unreacted monomers and SiO_2 nanoparticles. Furthermore, the front moved downward steadily without bubbles

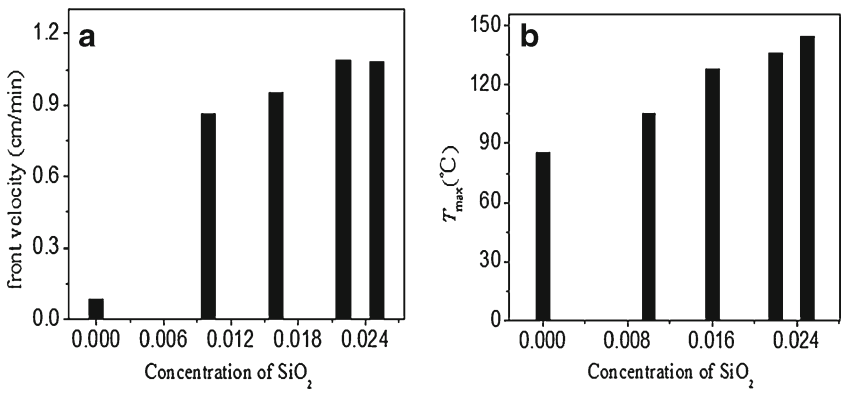

Fig. 4 Influence of SiO_2 nanoparticles on V_f (**a**) and T_{max} (**b**) during the preparation of the PAA/SiO_2 hybrid hydrogels

with the increase in time. No "finger phenomenon" was observed [10].

As we all know, it is an important features of FP without simultaneous spontaneous polymerization (SP) that the front velocity remains a constant [13, 14]. Figure 3a shows a typical curve for the front position as a function of time. As it can be seen, the experimental data was well fitted by a straight line, meaning that the front velocity was a constant, 0.95 cm/min. This indicated that the pure FP had occurred. Moreover, a typical temperature profile was obtained during the FP experiments as shown in Fig. 3b. The temperature remained constant until the front reached its junction, indicating SP was not occurring simultaneously [15].

The influence of concentration of SiO_2 nanoparticles on V_f and T_{max} is also shown in Fig. 4. It was found that V_f increased from 0.08 to 1.09 cm min^{-1} as the concentration of SiO_2 nanoparticles increased from 0 to 0.025 g mL^{-1}. The increase in the concentration of SiO_2 nanoparticles also caused the increase in T_{max} from 85 to 144 °C, which was similar to the front velocity trend. This may be attributed to the fact that more SiO_2 nanoparticles could increase the liquid viscosity of reaction mixture and would result in a higher front temperature. Therefore, the higher the polymerization temperature was, the quicker the V_f was. Similar results are reported in a previous research [22].

Characterization of PAA/SiO_2 hybrid hydrogels

Figure 5 is the SEM micrographs of the prepared FP2 hydrogel. It could be seen that the white circular paeticles in the SEM micrographs were the SiO_2 inorganic nanoparticles. The black background was the hydrogel matrix. We could not see the porous structures in the present SEM micrographs because the hydrogel network was in a collapsed (impact) status. In the preparation procedure of the hydrogel, the dry method has an important effect on the morphology of the hydrogel. In general, the hydrogel network is in a collapsed (impact) status when it is dried by a thermal air-drying method. Therefore, smooth (impact), nonporous structure is often observed in this case. However, the hydrogel network is in a swelling (loose) status when it is dried by a frozen dry method. The porous structure of the hydrogel remained because of water sublimate in the form of ice crystal. Thus, the porous structure is often observed [23]. In our experiment, although the equilibrium-swollen gels were frozen by liquid nitrogen for 6 h, the frozen dried results of liquid nitrogen is not good. Thus, the equilibrium-swollen gels were reduced in a collapsed (impact) status because the water in the hydrogel disappeared and dried in air. Therefore, smooth (impact), nonporous structure was observed. Similar results were seen in our previous reports [24]. In addition, it can be seen that nanosized SiO_2 particles with an average diameter of about 500 nm were dispersed in the hydrogel well. The distribution of SiO_2 nanoparticles in the PAA hydrogel was highly homogeneous without aggregation. This may be attributed to the fact that monomers polymerized rapidly and SiO_2 nanoparticles fast locked into the hydrogel networks were formed, which was also one of the obvious advantages of in situ FP. Figure 6 shows the FTIR spectra of PAA and PAA/SiO_2 hybrid hydrogels. It can be observed that the band with a weak shoulder at 2,926 and a medium band at 1,459 cm^{-1} belonged to the stretching of aliphatic –CH_2– and –CHR– groups, respectively. The characteristic absorption peak around

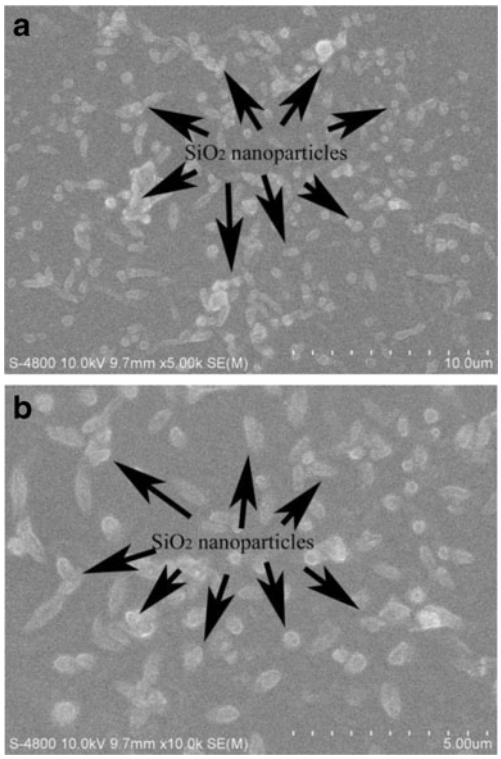

Fig. 5 SEM micrographs of the FP2 hydrogel. Magnification, **a** ×5,000 and **b** ×10,000

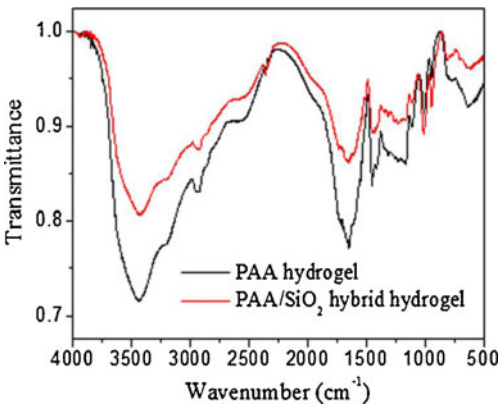

Fig. 6 FTIR spectra of PAA and PAA/SiO_2 hybrid hydrogels prepared by in situ FP

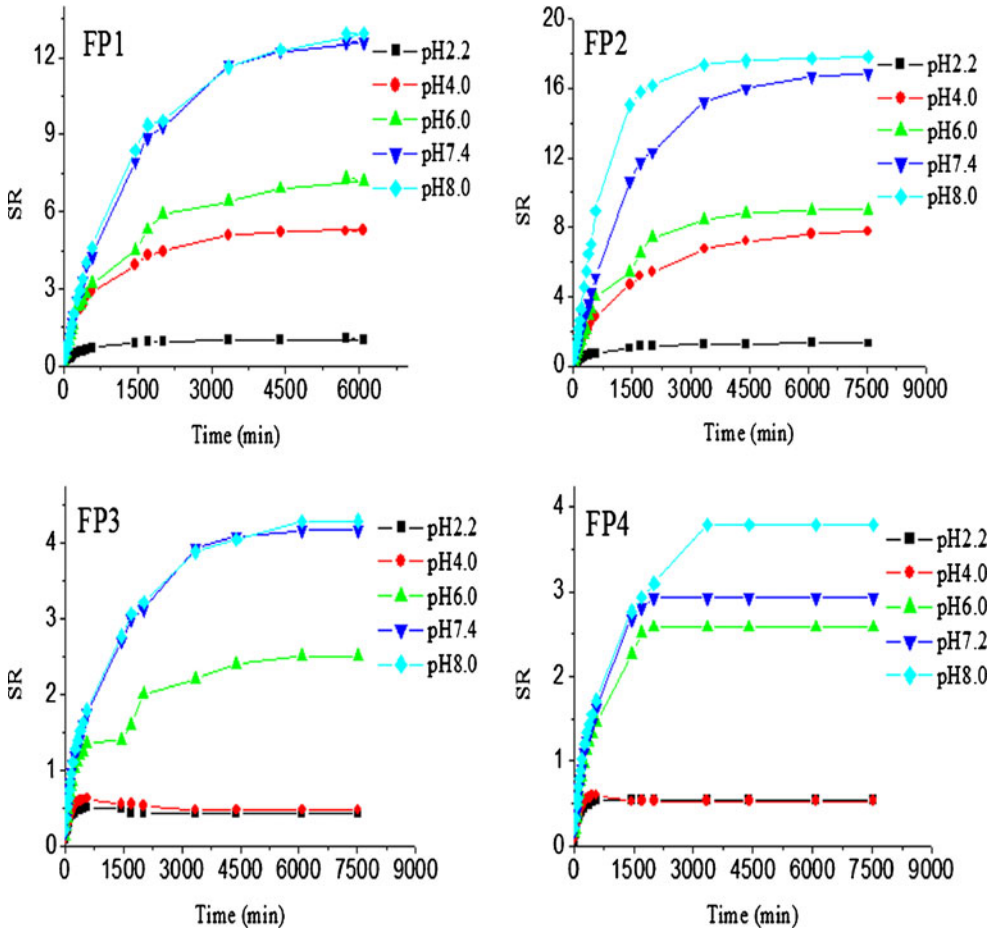

Fig. 7 Swelling kinetics of AA/SiO_2 hybrid hydrogels in different pH values of buffer solutions

3,400 cm^{-1} assigned to the $–NH_2$ and –OH groups could be observed in both PAA and PAA/SiO_2 hybrid hydrogels. In comparing the FTIR spectra of the PAA/SiO_2 hybrid hydrogel and PAA hydrogel, it was found that the intensity of the characteristic absorption peak around 3,400 and 1,600 cm^{-1} dramatically decreased in PAA/ SiO_2 hybrid hydrogel because of the existence of SiO_2 nanoparticles.

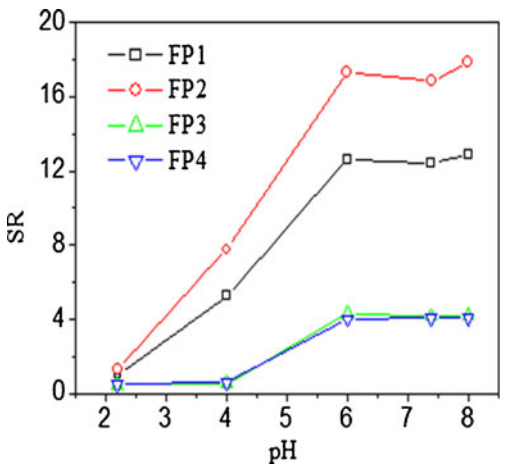

Fig. 8 Plot of the SR versus pH values of the buffered solutions

PH-sensitive swelling behaviors of PAA/SiO_2 hybrid hydrogels

To investigate the pH sensitivity of PAA/SiO_2 hybrid hydrogels, the swelling kinetics of the hydrogels in various pH values ranging from 2.2 to 8.0 were studied, respectively. As shown

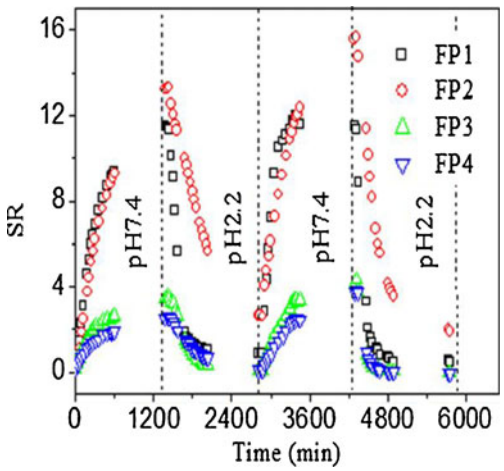

Fig. 9 Swelling/deswelling of hybrid hydrogels as a function of times in pH 2.2 and 7.4 buffer solution

Table 2 Compressive strength and equilibrium SR of hydrogels

Sample	Compressive strength (Ss; kPa)	Equilibrium SR (pH=8.0)	Appearance after test
FP0	12.6	12.1	Fractured
FP1	18.3	12.9	Fractured
FP2	35.5	17.8	Recovered
FP3	42.6	4.2	Recovered
FP4	41.9	4.1	Recovered

in Fig. 7, for every hybrid hydrogel, the SR of hydrogel increased with the increase in pH values. At the same pH values, the SR of hybrid hydrogels first increased with the increase in content of SiO_2 nanoparticles (see FP1 and FP2 hydrogels). This is perhaps because the SiO_2 nanoparticles dispersed in FP2 was much better than that in FP1 and was more proper for the water absorbency. However, when the content of SiO_2 nanoparticles continued to increase, a decrease in SR can be observed (see FP3 and FP4 hydrogels). It is probable because the hydrogel networks became impact and thicker in these cases, which is not suitable for water absorbency [25, 26].

The influence of pH values on the equilibrium SR of hybrid hydrogels was determined in different pH buffer solutions (i.e., 2.2, 4, 6, 7.4, and 8.0) at 25 °C. Figure 8 shows the change of the equilibrium SR of hybrid hydrogels with pH. Obviously, for all hybrid hydrogels, the equilibrium SR showed a sharp increase when the pH value changed from 2.2 to 6.0. This is mainly attributed to the ionization of carboxyl groups [6]. Furthermore, the ability of sharp increase in SR is parallel to the trend of swelling kinetics stated above.

Figure 9 shows the reversible pH-dependent swelling behaviors of the hybrid hydrogels in the pH 2.2 and 7.4 buffer solutions. When the hybrid hydrogels were first placed in pH 7.4 buffer solution, they swelled to a great degree because of the electrostatic repulsion among the ionized carboxyl groups of hydrogels. When the hybrid hydrogels were transferred into pH 2.2 buffer solution, the ionized carboxyl groups of hydrogels patted to proton. The hybrid hydrogels shrunk gradually due to the hydrogen bonding interaction between the non-ionized carboxyl groups [6]. For all hybrid hydrogels, the sudden and sharp swelling–deswelling behavior in different pH buffer solutions implied that they have high pH sensitivity and can be used for tailoring pulsatile (on–off swelling behavior) drug delivery. Here, inspection of FP2, especially, shows a continuous increase in variation (dynamic range) of SR with time. The main reason may be that the equilibrium SR of FP2 hydrogel was highest in all hybrid hydrogels because of its unique structure. The macromolecular chain of FP2 hydrogel was easier to relax than other hybrid hydrogels when the ionized carboxyl groups of hydrogels patted to proton [6]. In addition, after a cycle of reversible swelling–deswelling, all hybrid hydrogels were stable enough, which can be attributed that the introduction of SiO_2 nanoparticles can improve the mechanical strength of the PAA hydrogel.

Mechanical properties of PAA/SiO_2 hybrid hydrogels

The influence of different content of SiO_2 nanoparticles on the mechanical properties of the hybrid hydrogels were further investigated (Table 2). As shown in Table 2, as a result, the compressive strength of hyrogel increased with the increase in content of SiO_2 nanoparticles. The maximum of compressive strength of hyrogel may reach 42.6 kPa (FP3 hybrid hydrogel). In comparison, the compressive strength of a pure PAA hydrogel only reached 12.1 kPa. It appeared that the SiO_2 nanoparticles played an important role in enhancing the compressive strength of PAA hydrogels. For FP2 hybrid hydrogel, the compressive strength was the second highest among all hydrogels and remained a high-equilibrium SR. Figure 10

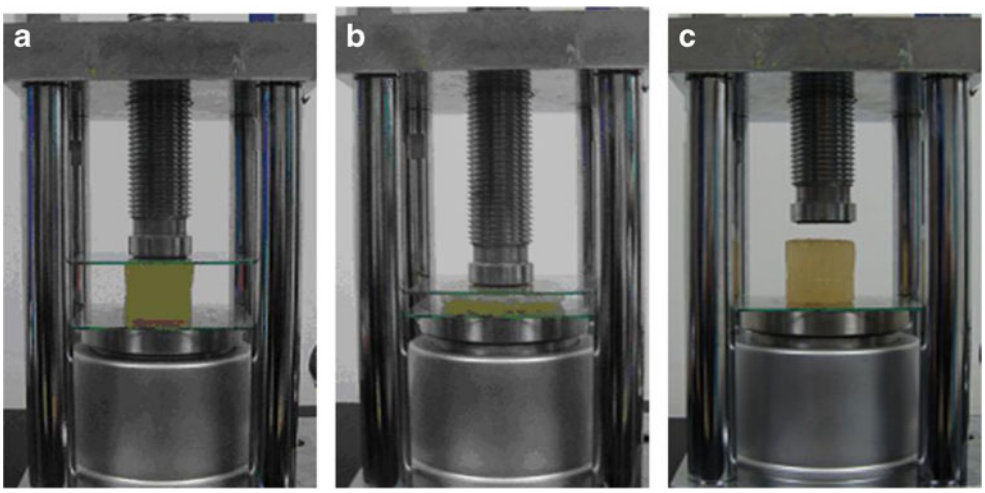

Fig. 10 Photographs of the swollen FP2 hybrid hydrogel **a** before, **b** during, and after compression test **c**

shows the photographs of FP2 hybrid hydrogel before compression test, during test, and after test, respectively. Interestingly, during the tests, FP2 hybrid hydrogel did not break, even under extreme high straining, and quickly recovered its original shape after the release of its load. This phenomenon also indicated that good hybrid hydrogels with high compressive strength in swollen status could be obtained via simple in situ FP technique. However, although the compressive strength of the hybrid hydrogels was high, too high content of SiO_2 nanoparticles also led to a decrease in the equilibrium SR of the hydrogel (FP3 and FP4 hybrid hydrogels).

Conclusions

In this study, high pH-sensitive PAA/SiO_2 hybrid hydrogels with high strength were rapidly prepared by in situ FP. The data of front velocity and front temperature implied that the pure FP had occurred. The rapid conversion reaction of monomer into the PAA hydrogel via the in situ FP could effectively avoid the precipitation of SiO_2 nanoparticles during FP. The increase in the concentration of SiO_2 nanoparticles led to an increase of V_f and T_{max}. For all hybrid hydrogels, the equilibrium SR showed a sharp increase when the pH value changed from 2.2 to 6.0, which was attributed to the ionization of carboxyl groups. After a cycle of reversible swelling–deswelling, all hybrid hydrogels were stable enough. The compressive experiments results indicated that the incorporation of SiO_2 nanoparticles into the PAA hydrogel may enhance the strength of the hydrogels.

Acknowledgments The authors are grateful to the science research project of Hubei Provincial Department of Education (grant no. D20123001) and Hubei Key Laboratory of Mine Environmental Pollution Control and Remediation (grant no. 2012101), and Innovative Team (grant no. T201323) of Hubei Polytechnic University for the financial support on this work.

References

1. Roy D, Cambre J, Sumerlin B (2010) Prog Polym Sci 35:278
2. Horkay F, Han M, Han I, Bang I, Magda J (2006) Polymer 47:7335
3. Jin X, Hsieh Y (2005) Polymer 14:5149
4. Tang Q, Sun X, Li Q, Wu J, Lin J (2009) J Colloid Interface Sci 339:45
5. Tang Q, Sun X, Li Q, Wu J, Lin J (2009) J Colloid Interface Sci 346:91
6. Li S, Li H, Yang Y, Yang X, Xu H (2007) J Appl Polym Sci 106:3792
7. Wu Q, Zhou C (2011) Colloids Surf A: Biointerface 84:155
8. Wang N, Han Y, Liu Y, Bai T, Gao H, Zhang P, Wang W, Liu W (2012) J Hazard Mater 213–214:258
9. Qin X, Zhao F, Liu Y, Feng S (2011) Eur Polym J 47:1903
10. Pojman JA (1991) J Am Chem Soc 113:6284
11. Fiori S, Mariani A, Ricco L, Russo S (2003) Macromolecules 36:2674
12. Fang Y, Chen L, Chen S (2009) J Polym Sci Part A: Polym Chem 47:1136
13. Yan Q, Lu G, Zhang W, Ma X, Ge CC (2007) Adv Funct Mater 17:3355
14. Hu T, Fang Y, Yu H, Chen L, Chen S (2007) Colloid Polym Sci 285:891
15. Cui Y, Yang J, Zhan Y, Zeng Z, Chen Y (2008) Colloid Polym Sci 286:97
16. Alzari V, Monticelli O, Nuvoli D, Kenny J, Mariani A (2009) Biomacromolecules 10:2672
17. Yu C, Zhou J, Wang C, Chen L, Chen S (2010) J Polym Sci Part A: Polym Chem 48:2000
18. Liu N, Shao H, Wang C, Chen Q, Chen S (2013) Colloid Polym Sci. 291:1871
19. Feng Q, Li F, Yan Q, Zhu Y, Ge C (2010) Colloid Polym Sci 288:915
20. Feng Q, Yan Q, Ge C (2013) Colloid Polym Sci 291:1163
21. Li S, Zhang H, Feng J, Xu R, Liu X (2011) Desalination 280:95
22. Sanna R, Sanna D, Alzari V, Nuvoli D, Scognamillo S, Piccinini M, Lazzari M, Gioffredi E, Malucelli, Mariani A (2012) J Polym Sci Part A: Polym Chem 50:4110
23. Kang H, Tabata Y, Ikada Y (1999) Biomaterials 20:355
24. Li S, Huang H, Tao M, Liu X, Cheng T (2013) J Appl Polym Sci 129:3737
25. Garnweitner G, Smarsly B, Assink R (2003) J Am Chem Soc 125:5626
26. Liu H, Huang C, Teng X, Wang H (2008) Mater Sci Eng, A 487:258